Effects of thermal annealing of segmented-polyurethane on surface properties, structure and antithrombogenicity

ATSUO TAKAHASHI[1,2], RIO KITA[2], MAKOTO KAIBARA[2,*]
[1]*Department of Physics, Faculty of Science, Science University of Tokyo, Shinjuku, Tokyo 162-0825, Japan*
[2]*Supramolecular Science Laboratory, RIKEN (The Institute of Physical and Chemical Research), Wako, Saitama 351-0198, Japan*
E-mail: kaibara@postman.riken.go.jp

Analyses of the surface structure and properties of thermally heat-treated and non-treated segmented-polyurethane (SPU) surfaces showed that a crystalline structure, the domain size of which was larger than that of the micro-phase separation structure, appeared when the SPU surface was annealed in the temperature range of 60–140 °C. The appearance of the crystalline structure resulted in a decrease in surface free energy, that is, an increase in the hydrophobicity of the surface. Whole blood or platelet-rich plasma (PRP), when in contact with a SPU surface, which had previously been in contact with a glass surface during casting, coagulation of the whole blood occurred within approximately 30 min and, in case of PRP, in approximately 60 min. When the SPU surface was modified by thermal annealing, the coagulation time for PRP was delayed, whereas that of whole blood remained essentially unchanged. Relationships between the surface properties and the structure of annealed SPU and antithrombogenicity are discussed. The data collected herein suggest that the heat treatment of SPU might be useful for improving antithrombogenicity.

1. Introduction

Antithrombogenic material surfaces are required for developing artificial organs which are in contact with blood. For example, in the development of artificial vascular grafts, the primary failure of a small caliber synthetic vascular graft involves thrombus formation in the short term. In the long term, intimal hyperplasia, caused by compliance mismatch between the graft and host tissue, represents the main cause for failure.

Commercially available synthetic grafts, which are currently in use, are composed of polyethyleneterephtalate (PET) [1] and polytetrafluoroethylene (PTFE) [2–4], both of which are relatively rigid polymers. These grafts are effective for the replacement of large arteries but frequently fail in the case of a smaller diameter vascular graft, such as a coronary artery. The use of elastic polymers such as polyurethane would be expected to overcome this compliance mismatch, in part [5]. At present, however, no polymers that are able to provide a sufficiently antithrombogenic surface are available for this purpose.

It is well known that segmented-polyurethane (SPU) represents an antithrombogenic and biocompatible polymer and has been widely used in the development of a variety of artificial organs [6, 7]. In these cases, SPU is fabricated in the form of films and tubes or is used directly as a material. Numerous investigations have been reported on surface modification with the goal of improving the antithrombogenicity and to control cell adhesion. When the surface of SPU, where endothelial cells are not capable of proliferating, is modified by ion-implantation [8], plasma-treatment [9] or carbon-deposition [10, 11], the adhesion and proliferation of endothelial cells can be drastically improved. However, all of these methods require some special apparatus. The thermal annealing of SPU, a simple and convenient technique, has been performed to form compliant vascular grafts as well as in investigations of thermal stability including micro-phase separation, glass transition and structural changes [12].

The molecular structure of polyether-urethane consists of soft polyether segments and hard urethane segments. The domain structure, which is formed on the surface of the polyurethane, is capable of biological responses, which include antithrombogenic activity and low platelet activation [13]. The surface structure and properties of SPU would be expected to be dependent on the materials

*Author to whom all correspondence should be addressed.

and atmosphere, which the SPU solution had been in contact during the casting procedure.

In the study described herein, in order to modify the SPU surface, a simple treatment, which involved thermal annealing, was carried out, and the surface properties, structure, and antithrombogenicity of the surface was examined.

2. Materials and methods

2.1. Polymer

Segmented-polyurethane (SPU, Pellethane 2363-80AE) obtained from the Dow Chemical Co. (Midland, MI, USA) was used in this study. The SPU consists of hard segment composed of 4,4′-methylene diphenyl diisocyanate (MDI) and butanediol (BDO), and soft segment composed of polytetramethyleneoxide (PTMO). In order to purify the SPU sample, it was dissolved in tetrahydrofurane (THF) and recrystallized via the addition of methyl alcohol. To prepare SPU films, SPU, dissolved in THF at a concentration of 2 wt %, was cast on a clean glass plate and then dried under a nitrogen atmosphere at room temperature. The film was then placed in a vacuum oven at 40 °C for more than 24 h. The dried SPU film was then gently detached from the glass plate. The thickness of these SPU films was about 100 μm. The SPU surface, which was in contact with air, is denoted as the air facing surface (AFS) and that facing the glass (substrate) as the substrate facing surface (SFS) in this paper.

Thermal annealing of the SPU film was performed at a fixed temperature between 60–180 °C for 1 h under a nitrogen atmosphere.

2.2. Analysis of mechanical and calorimetric properties

The dynamic storage modulus (E′) and loss modulus (E″) of SPU films were measured using a forced oscillation type rheometer (Rheolograph Solid, Toyo Seiki Seisaku-Sho Ltd., Tokyo, Japan), operating at 10 Hz at a heating rate of 4 °C min^{-1} in a temperature range from − 190 to + 100 °C. Differential scanning calorimetry (DSC) measurement was performed using a model DSC8230B (Rigaku Denki Co., Ltd, Tokyo, Japan) in an argon atmosphere. The thermogram for SPU sample was measured at a heating rate of 20 °C min^{-1} in a temperature range from 20 to 250 °C.

2.3. Analysis of SPU surfaces

The SPU-distilled water–air contact angle was measured with a contact angle meter (FACE CA-X, Kyowa Kaimen Kagaku Co., Ltd., Saitama, Japan) at 25 °C.

The surface morphology of SPU films was observed with a tapping mode AFM (Nanoscope III, Digital Instrument, inc., Santa Barbara, CA, USA), where height and phase imaging data were obtained simultaneously.

2.4. Analysis of antithrombogenicity of SPU surface

The coagulation process of a blood sample in a cone-shaped cup (diameter: 20 mm, cone angle: approximately 40°), which was prepared from SPU film, was monitored using a damped oscillation rheometer. This rheometer has been described in detail elsewhere [14]. The change in logarithmic damping factor (LDF) of a blood sample in the sample cup can be sensitively detected by the rheometer. The LDF value is closely related to the viscosity and viscoelasticity of the blood sample. The coagulation time of blood sample is determined from the initial change in the LDF value.

Blood samples were obtained from human adult volunteers by venepuncture using a 1/10 volume of 3.8% tri-sodium citrate. The coagulation reaction was initiated by adding 85 μl of a 0.25 M $CaCl_2$ solution to 1 ml of the blood sample.

3. Results

3.1. Mechanical and thermal properties of annealed SPU

Fig. 1 shows the temperature dependence of E′ and E″ for the control SPU and SPU annealed at 150 °C. The relaxation of around − 140 °C can be attributed to the local mode relaxation of the main chain of a soft

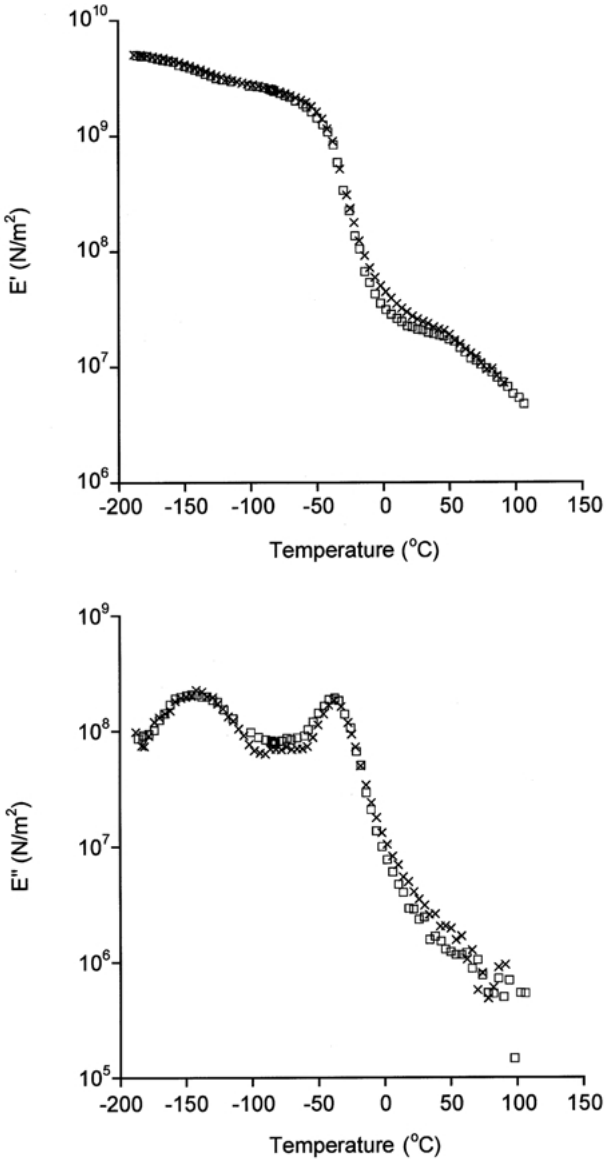

Figure 1 Dynamic storage modulus E′ and loss modulus E″ of the control SPU (×) and SPU annealed for 60 min at 150 °C (□).

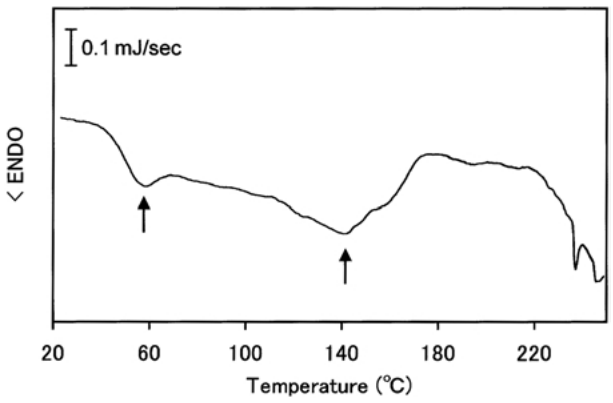

Figure 2 DSC thermogram of the control SPU measured at a heating rate of 20 °C min^{-1}.

segment, and that around -40 °C to the glass transition of the soft segment [15–17]. The temperature dependence of E′ and E″ for the annealed SPU was in good agreement with that obtained for the control SPU. The stress–strain relationship for the annealed SPU was also in agreement with that for the control SPU (data not shown).

Fig. 2 shows the DSC thermogram of the control SPU. An endothermic peak around 60 °C is associated with the glass transition of a hard segment of SPU and that at around 140 °C with the melting of a hard segment, which are consistent with data reported by Martin *et al*. [15].

3.2. Surface properties

Fig. 3 shows the water contact angle of the control AFS and SFS, and the annealed SFS plotted as a function of thermal annealing temperature. The contact angle of the control SFS (at 40 °C) was smaller than that of the control AFS. The contact angle of the annealed SFS was higher than that of the control AFS, and the values for SFS initially increased and then decreased, passing through a maximum, with increasing annealing temperatures.

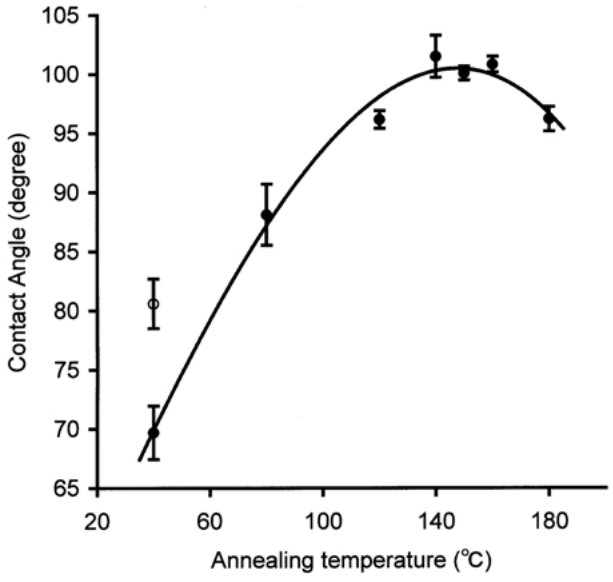

Figure 3 Annealing temperature dependence of water contact angle on SFS and AFS of SPU. ○; AFS, ●; SFS. The error bars indicate standard deviations.

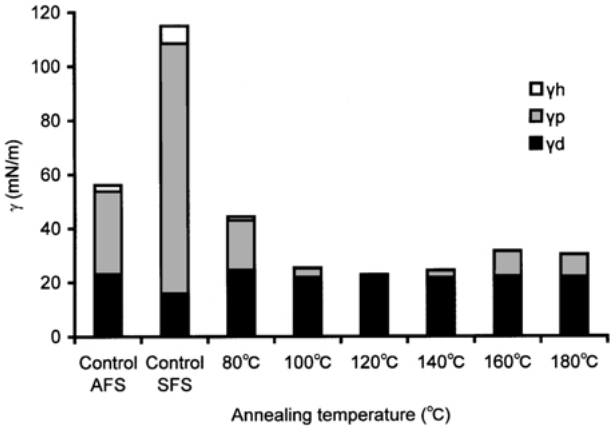

Figure 4 Surface free energy for the control AFS and SFS, and SFS annealed at different temperature. γ^d, γ^p and γ^h mean dispersion (nonpolar), polar and hydrogen bond components, respectively.

The surface free energy of the SPU films was evaluated using contact angle measurements, according to an extended Fowkes equation [18]. The surface free energy (γ) can be expressed as follows:

$$\gamma = \gamma^d + \gamma^p + \gamma^h \quad (1)$$

where γ^d is from the dispersion (nonpolar) component, γ^p the polar component and γ^h the hydrogen bond component. To determine the total surface free energy and the energy of each respective component, three different liquids, methylene iodide, *n*-hexadecane and glycerol, the surface free energies of which are known, were used.

Fig. 4 shows the values of total free energy (γ) and its components for the control AFS and SFS, and SFS annealed at different temperatures. The value of γ for the control SFS was twice as large as that of the control AFS. The value of γ for the SFS decreased with increasing annealing temperature, up to 120 °C. A further increase in annealing temperature led to an increase in γ. The annealing of SFS resulted in an increase in the dispersion component, but the value was nearly independent of the annealing temperature. The polar component was largely decreased by annealing up to the melting temperature (T_m : 140 °C) of the hard segment and then increased slightly. The hydrogen component decreased as the result of annealing and almost disappeared at temperatures above 100 °C.

3.3. Surface morphology of SPU

Fig. 5 shows topological (A) and phase (B) imaging photographs of the control SFS. A micro-phase structure was clearly observed by phase imaging, which was independent of the height distribution. A power spectrum obtained by Fast Fourier Transformation analysis of the phase imaging data showed a characteristic micro-phase separated structure with a repeated period of 25 nm, which is consistent with that obtained by AFM analysis of a similar SPU sample [19].

Phase imaging photographs of SFS, which had been annealed at different temperatures are shown in Fig. 6. When the SPU was thermally annealed in the temperature range of 80–140 °C, a crystalline structure,

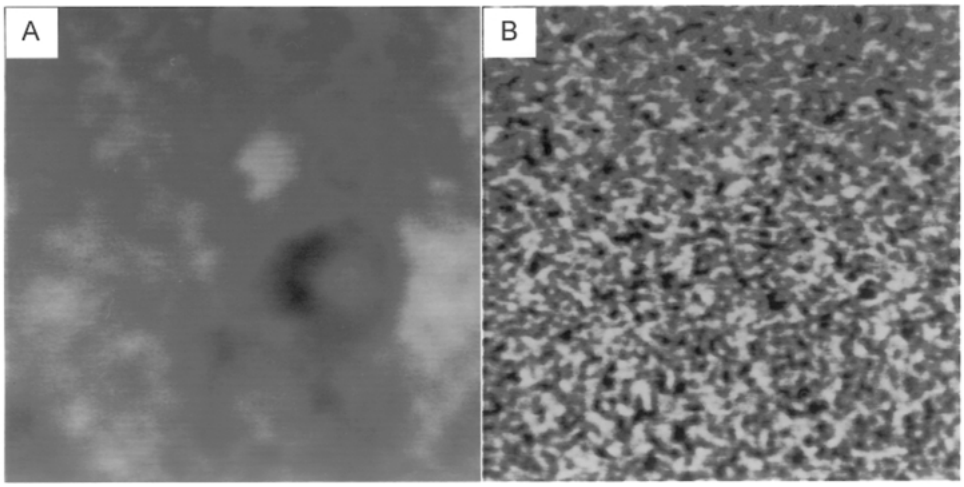

Figure 5 Topographical (A) and phase (B) imaging photographs for the control SFS. Topographical and phase scale are 0–10 nm and 0°–10°, respectively. The scan width was 500 nm.

domain size of which was larger than that of the microphase separated structure, appeared. The amount of crystalline domain (bright area in Fig. 6C–F) appears to increase with increasing annealing temperature. Beyond 150 °C, the structure of the crystalline domain crumbled.

3.4. Antithrombogenicity of the SPU surface

Fig. 7 shows the coagulation time (*Ti*) for whole blood and PRP, in contact with the control SFS and AFS, and a SFS that had been annealed for 60 min at 150 °C. In all surfaces, the values of *Ti* for the PRP were larger than for whole blood. In the case of whole blood, the value of *Ti* for the control SFS was smaller than that for the control AFS. The thermal annealing of SFS resulted in a slight delay in coagulation time for whole blood, but the difference in the values of *Ti* between the control AFS and the annealed SFS was negligible. In the case of PRP, the values of *Ti* for the control AFS and SFS were larger than that for whole blood, and the annealing of SFS resulted in a delay in the initiation of coagulation.

Fig. 8 shows the relative coagulation time of PRP, in

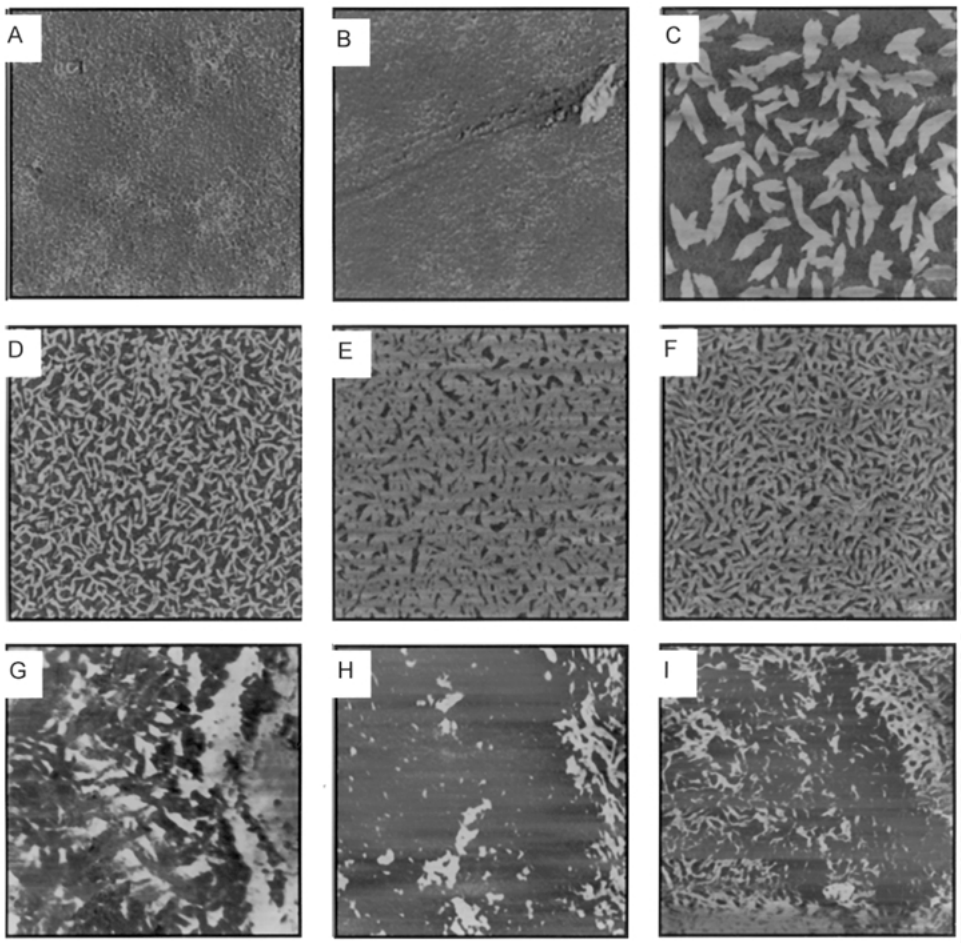

Figure 6 Annealing temperature dependence of phase imaging photographs for SFS. The annealing temperatures (°C) are: (A) control, (B) 60, (C) 80, (D) 100, (E) 120, (F) 140, (G) 150, (H) 160, (I) 180. In all images, the phase scale is 0–60°, with a scan size of $3 \times 3\,\mu m^2$.

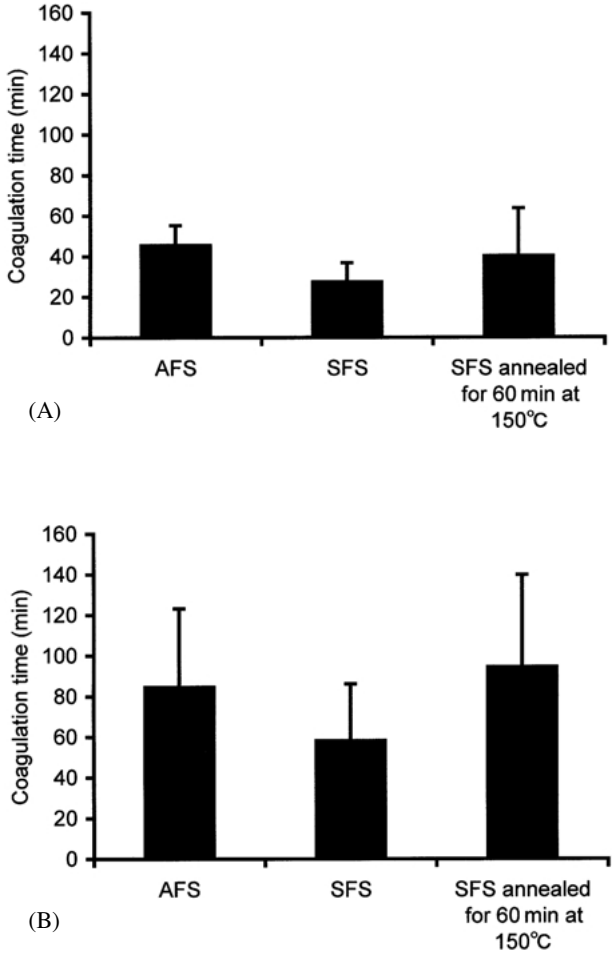

Figure 7 Coagulation time for whole blood (A) and PRP (B) in contact with the control AFS and SFS, and the annealed SFS for 60 min at 150 °C.

contact with the annealed SFS, plotted against annealing temperature. The value of PRP was 1.5 times larger than that of the control, when the annealing was performed in the temperature range of 100–140 °C, but, at temperatures above 150 °C the values gradually decreased and approached the control value at higher temperatures of around 180 °C.

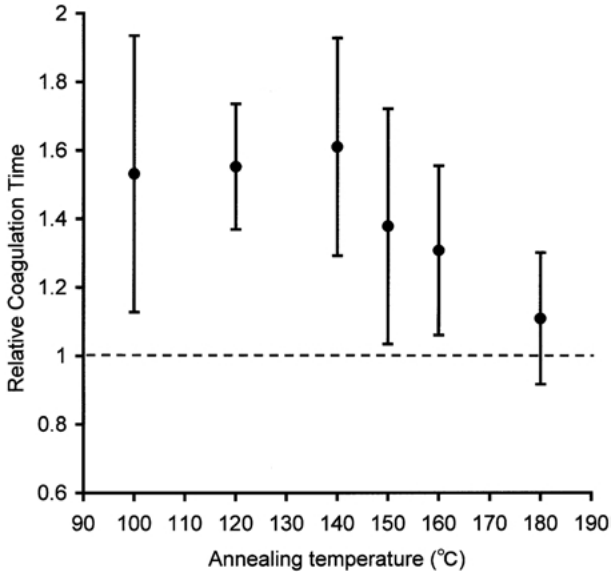

Figure 8 Annealing temperature dependence of the relative coagulation time of PRP in contact with the annealed SFS. Relative coagulation time indicates the ratio of coagulation time for the annealed SFS to that of the control. An error bar represents the standard deviation.

4. Discussion

The temperature dependence of E′ and E″ for SPU annealed for 60 min at a temperature of 150 °C coincided well with that of the control SPU (Fig. 1). The stress–strain relationship of the SPU, annealed at the same conditions, also coincided with that of the control (data not shown). The results suggest that the bulk mechanical properties of SPU remained unchanged as a result of the thermal treatment under the present annealing conditions.

When a SPU solution is cast on a glass surface under conditions of slow solvent evaporation, the domain structure of SPU surface would be arranged so as to minimize the surface free energy. From Fig. 4, it is clear that the AFS had a larger dispersion component and lower polar and hydrogen bond components, when compared with that of the SFS. Since the soft segment in SPU has a methylene sequence, in the form of PTMO, which is hydrophobic and has a low surface free energy, it is assumed that the soft segment is concentrated on the AFS. On the contrary, since the hard segment possesses π-electronic benzene, carbonyl and amino acid groups, which constitute polar and hydrogen bond components, this portion of the polymer may be concentrated on the SFS.

The mechanism of the formation of the crystalline structure of SFS, when SPU is annealed in the temperature range from 80 to 140 °C, remains unclear. Since the melting point of the soft segment is about 30–40 °C [20, 21], the glass transition of the hard segment is near 60 °C, and the melting point of hard segment is in the vicinity of 143 °C (Fig. 2), it can reasonably be assumed that the crystalline structure was formed in co-operation with the thermal motion of the hard segment and the deposition of the soft segment in a nitrogen atmosphere, and that a highly concentrated soft segment surface may, in fact, form a crystalline structure. Therefore, the total surface free energy of SFS would be expected to decrease with an increase in annealing temperatures, up to 140 °C.

A further increase in annealing temperature resulted in a slight increase in the total free energy, where the polar component increased, but the dispersion component was nearly independent of the annealing temperature. In addition, the hydrophobicity slightly decreased at temperatures higher than 140 °C (Fig. 3). The destruction of the crystalline structure at temperatures above 140 °C (Fig. 7) may result in the movement of the hard segment to the SFS, which may be due to the dissolution and mixing of soft and hard segments.

In our previous study, we showed that platelet-free plasma (PFP, having no cellular components), when placed in a simple vascular model tube composed of a glass tube and a bovine aortic endothelial cell monolayer, did not coagulate during the duration of the measuring period of over 150 min, indicating that the intrinsic and extrinsic coagulation pathways are not activated in the model tube [22]. On the contrary, whole blood in the tube

began to coagulate at about 30 min and PRP at 50–60 min. The coagulation of whole blood was observed to occur in any inert surfaces against blood coagulation. The triggering mechanism for coagulation is largely due to the activation of factor IX by erythrocytes in blood under stagnant flow conditions [22]. Therefore, the small differences in *Ti* values for whole blood in contact with the control AFS and SFS, and the annealed SFS (Fig. 7a) suggests that the coagulation of whole blood is governed by the activation of F-IX by erythrocytes and not as the result of an interaction with SPU surface and other blood components, such as platelet or leukocytes.

In a previous study, it was also shown that the coagulation of whole blood and PRP, in contact with a collagen surface, occurred rapidly, compared to samples in the model tube described above and the SPU tube, whereas PFP, in contact with a collagen surface did not coagulate [23]. In addition, more aggregated platelets, adhered to the collagen surface, were observed. This suggests that activated platelets provide an alternative pathway by-passing factor XII for initiating intrinsic coagulation [24]. The number of platelets adhering to the SFS was approximately four times that of the AFS when compared at 30 min after the start of the measurement (data not shown). The coagulation of PRP in contact with the control AFS was delayed, compared to that of the control SFS (Fig. 7b). This suggests that platelets that have adhered to the AFS are less active than those adhered to the SFS surface. The coagulation of PRP in contact with the annealed SFS at a temperature up to 140 °C was considerably delayed, compared to that of the control SFS and AFS (Fig. 8). This suggests that the annealing of SFS results in the development of a hydrophobic surface and, prevents the activation of adhered platelets. The shortened coagulation time of PRP, in contact with SFS treated at a temperature above 150 °C, may due to a decrease in the hydrophobicity of SFS.

5. Conclusion

The present data indicates that thermal treatment is advantageous in improving the antithrombogenicity of a substrate facing surface of SPU. The annealing temperature resulting in the most antithrombogenic surface for SPU is predicted to be between the glass transition (60 °C) and melting point (143 °C) of hard segment. In this temperature range, a crystalline structure was produced, which resulting an increase in hydrophobicity of the SPU surface, resulting in antithrombogenicity.

Acknowledgment

We are grateful to Dr. Toshiyuki Shibata (RIKEN, The Institute of Physical and Chemical Research) who generously permitted us to use the differential scanning calorimetry.

References

1. S. SCHMIDT, T. HUNTER, W. SHARP, G. MALINDZAK and M. EVANCHO, *J. Vasc. Surg.* **1** (1984) 434.
2. K. KESLER, M. HERRING, M. ARNOLD, J. GLOVER, H. PARK, M. HELMUS and P. BENDICK, *ibid.* **3** (1986) 58.
3. J. BUDD, K. ALLEN and P. BELL, *Br. J. Surg.* **78** (1991) 878.
4. L. POOLEWARREN, K. SCHINDHELM, A. GRAHAM, P. SLOWIACZEK and K. NOBLE, *J. Biomed. Mater. Res.* **30** (1996) 221.
5. K. HAYASHI, K. TAKAMIZAWA, T. SAITO, K. KIRA, K. HIRAMATSU and K. KONDO, *ibid.* **23** (1989) 229.
6. T. HOW and R. CLARKE, *J. Biomech.* **17** (1984) 597.
7. F. BIESTER, D. BEHREND and H. KLINKMANN, *Int. J. Artif. Organs* **5** (1982) 191.
8. M. IWAKI, A. NAKAO, M. KAIBARA, H. SASABE, S. KANEKO, H. NAKAJIMA, Y. SUZUKI, M. KUSAKABE and T. FUJIHANA, *Nucl. Instrum. Meth. Phys. Res.* **106** (1995) 618.
9. Y. KAWAMOTO, A. NAKAO, Y. ITO, N. WADA and M. KAIBARA, *J. Mater. Sci. Mater. Med.* **8** (1997) 551.
10. M. KAIBARA, Y. KAWAMOTO, S. YANAGIDA and S. KAWAKAMI, *Biomaterials* **16** (1995) 1229.
11. M. KAIBARA, H. IWATA, H. WADA, Y. KAWAMOTO, M. IWAKI and Y. SUZUKI, *J. Biomed. Mater. Res.* **31** (1996) 429.
12. A. MORI, Y. IMANISHI, T. ITO and K. SAKAOKU, *Biomaterials* **6** (1985) 325
13. K. KATAOKA, T. OKANO, T. AKAIKE, Y. SAKURAI, T. NISHIMURA, M. MAEDA, Y. NITADORI, T. TSURUTA, M. SHIMADA and I. SHINOHARA, in ''Advances in Biomaterials'', vol. 3 (Winter, Gibbons & Plenk Jr, New York, 1982) p. 493.
14. M. KAIBARA and M. DATE, *Biorheology* **22** (1985) 197.
15. D. J. MARTIN, G. F. MEIJS, P. A. GUNATILLAKE, S. P. YOZGHATLIAN and G. M. RENWICK, *J. Appl. Polym. Sci.* **71** (1999) 937.
16. A. TAKAHARA, J. TASHITA, T. KAJIYAMA and M. TAKAYANAGI, *J. Biomed. Mater. Res.* **19** (1985) 13.
17. B. E. READ and G. WILLIAMS, *Polymer* **2** (1961) 239.
18. T. HATA, Y. KITAZAKI and T. SAITO, *J. Adhesion* **21** (1987) 177.
19. R. S. MCLEAN and B. B. SAUER, *Macromolecules* **30** (1997) 8314.
20. R. E. WETTON and G. ALLEN, *Polymer* **7** (1966) 331.
21. G. W. MILLER and J. H. SAUNDERS, *J. Appl. Polym. Sci.* **13** (1969) 1277.
22. S. KAWAKAMI, M. KAIBARA, Y. KAWAMOTO and K. YAMANAKA, *Biorheology* **32** (1995) 521.
23. Y. KAWAMOTO and M. KAIBARA, *Blood Coagul. Fibrinolysis* **3** (1992) 371.
24. P. N. WALSH and J. H. GRIFFIN, *Blood* **57** (1981) 106.

Received 19 April
and accepted 3 September 2001